Transactions on Machine Intelligence 3(4) (2020) 218-225

ISSN Online: 2821-1693

Transactions on Machine Intelligence

Journal Homepage: https://tmachineintelligence.ir/index.php/TMI

Design and Simulation of a Single-Phase Grid-Connected Microinverter for Photovoltaic Systems

H. Hassanpour[1,*], M. Ehsanian[2]

[1] Electrical Engineering, K.N. Toosi University of Technology, Tehran, Iran
[2] Associate Professor, Department of Electronics, K.N. Toosi University of Technology, Tehran, Iran

ARTICLE INFO

Article History:
Received 3 August 2020
Received in revised form 10 October 2020
Accepted 9 December 2020
Available online 9 December 2020

Keywords:
Power Isolation, Photovoltaic Systems, Capacitor, Lifespan, Voltage Fluctuations, Second Harmonic Ripple

ABSTRACT

In single-phase grid-connected photovoltaic (PV) systems, maintaining a constant input power while dealing with a pulsating output power is a crucial challenge. This isolation is typically achieved using an energy storage element, most commonly a high-voltage DC link capacitor. The AC array structure of such systems consists of a single solar array connected to the grid through an inverter. Since the inverter's operational lifespan should align with that of the solar array, the choice of capacitor plays a critical role in system reliability. Electrolytic capacitors, despite their cost-effectiveness, exhibit a significantly shorter lifespan than solar arrays, necessitating the use of high-cost film capacitors with enhanced durability. A key challenge in designing the DC link voltage controller is mitigating voltage fluctuations in the capacitor and suppressing second harmonic ripple, both of which are inversely related to capacitor capacity and, consequently, system cost. Traditional approaches often require large capacitors to reduce these fluctuations, leading to increased cost and bulkiness. This paper proposes a digital control strategy for stabilizing the DC link capacitor voltage in single-phase grid-connected PV systems. The proposed method employs a low-pass finite impulse response (FIR) filter, which effectively suppresses voltage oscillations while maintaining system efficiency. The digital implementation of this controller enhances flexibility, reliability, and cost-effectiveness compared to conventional analog controllers. Simulation and experimental results demonstrate the effectiveness of the proposed approach in reducing voltage ripple and improving the stability of the DC link, thereby extending the lifespan of the inverter and enhancing overall system performance.

1. INTRODUCTION

The continuous increase in greenhouse gas emissions and growing concerns about global environmental protection, alongside rising energy demand, have led to a significant expansion in the use of various renewable energy sources [1-5]. Among renewable energy sources, solar energy is an appropriate choice for diverse applications, primarily because it can be directly converted into electrical energy using photovoltaic (PV) systems

* Corresponding Author: h.hassanpour@email.kntu.ac.ir
Electrical Engineering, K.N. Toosi University of Technology, Tehran, Iran

http://dx.doi.org/10.47176/TMI.2020.218

[6]. Grid-connected photovoltaic systems are connected to solar panels on one side and the grid on the other. Therefore, these systems must meet two essential requirements: operating the panels at their maximum power point (MPP) despite their nonlinear behavior, and injecting a pure sinusoidal current into the grid. As a result, several international standards for designing and constructing photovoltaic systems must be adhered to [7, 8].

Photovoltaic systems have various configurations. Among them, microinverters, shown in Figure 1, are low-power systems where the inverter is connected at the back of the solar panel. This makes these systems integrated, and therefore, the lifespan of the components used in the system is expected to be synchronized. However, electrolytic capacitors used in these systems are known for their short lifespan and are a serious limiting factor. The nominal lifespan of different capacitors varies, for example, around 1000 to 7000 hours at 105 degrees Celsius, whereas the lifespan of solar panels is 20 years or more, significantly exceeding that of electrolytic capacitors [9].

Among the various photovoltaic array configurations, microinverters are popular due to their numerous advantages, including high efficiency, system reliability, maximum power extraction capability, low installation cost, “Plug-N-Play” capability, increased modularity, and flexibility. The power level in these configurations is approximately 150 to 300 watts. As mentioned in the introduction, the mismatch in the lifespan of components used in microinverter-based photovoltaic systems and solar panels is a significant challenge. Since capacitors are used for power isolation in microinverters, the topic of power isolation and the capacity of capacitors used in these systems is crucial and will be addressed in the next section [10].

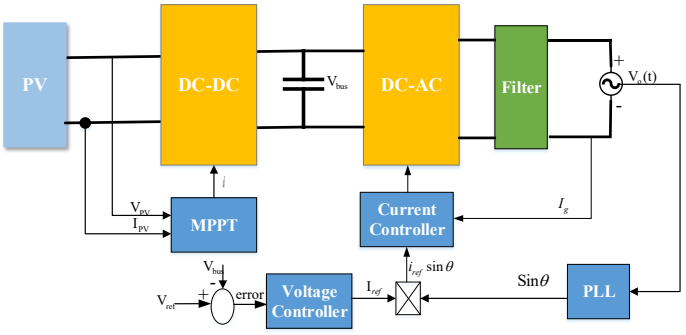

Fig.1. General Structure of a Photovoltaic System

2. STUDY OF SYSTEM DYNAMICS

If we neglect the power losses in the inverter and the power of the output filter, the input and output power of the inverter will be equal, as follows:

$$P_{i\_inverter} = P_{o\_inverter} \tag{1}$$

where $P_{\text{i\_inverter}}$ is the input power to the inverter and $P_{\text{o\_inverter}}$ is the output power from the inverter. On the other hand, we know that the inverter's output power is the same as the grid power, represented as:

$$P_g = v_g(t) i_g(t) = P_{o\_inverter} \tag{2}$$

where $v_g(t)$, $i_g(t)$, and P_g are the grid voltage, current, and power, respectively. If the power coming from the solar panel is denoted as P_{in}, then:

$$P_{in} = P_{bus} + P_{i\_inverter} \tag{3}$$

where P_{bus} is the power of the bus capacitor. By integrating the equations, we get:

$$P_{bus} = P_{in} - P_g \tag{4}$$

Moreover, the bus capacitor power can be derived from the following equation:

$$P_{bus} = C_{bus} V_{bus} \frac{dV_{bus}}{dt} \tag{5}$$

where C_{bus} is the capacitance and V_{bus} is the voltage across the capacitor. The stored energy in the capacitor can be considered as:

$$W_{bus} = \int P_{bus} dt = \frac{1}{2} C_{bus} V^2{}_{bus} \tag{6}$$

By expanding the stored energy, it can be written as:

$$W_{bus} = \frac{1}{2} C_{bus} V_{bus}{}^2 \approx \frac{1}{2} C_{bus} V_{ref}{}^2 + C_{bus} V_{ref} (V_{bus} - V_{ref}) \tag{7}$$

Based on these relationships, the dynamic loop of the inverter can be illustrated as in Figure 2-a. By employing approximations, the control loop is shown in Figure 2-b. As observed, this system is entirely linear.

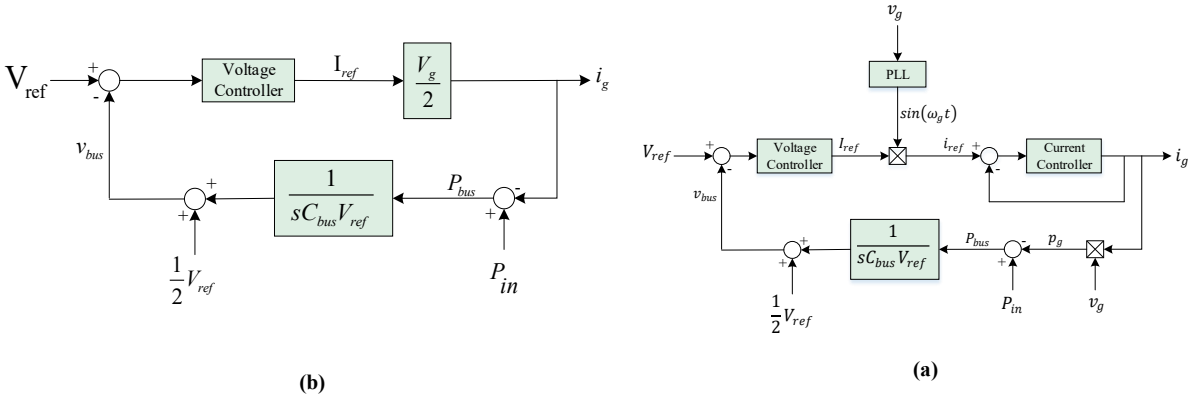

Fig. 2. Dynamic Loop of Grid-Connected Inverter. a- Non-linear b- Time-Invariant Linear

The characteristic equation of the control loop is:

$$1\text{-k}\frac{V_g}{2\text{C}_{\text{bus}}V_{\text{ref}}}(1+\frac{1}{\tau\text{s}})\frac{1}{s}=0 \tag{8}$$

By comparing the characteristic equation with the quadratic equation, we have:

$$\begin{cases} 2\xi\omega_n = \text{-k}\dfrac{V_g}{2\text{C}_{\text{bus}}V_{\text{ref}}} \\ \omega^2{}_n = \text{-k}\dfrac{V_g}{2\text{C}_{\text{bus}}V_{\text{ref}}\tau} = \dfrac{2\xi\omega_n}{\tau} \end{cases} \tag{9}$$

The response of the bus voltage to a step function is:

$$\begin{aligned} v_{\text{bus}}(t) &= \frac{1}{C_{\text{bus}}V_{\text{ref}}} \frac{s}{s^2+2\xi\omega_n s+\omega^2{}_n} \frac{P}{s} \\ &= \frac{P}{C_{\text{bus}}V_{\text{ref}}\omega_n\sqrt{1-\xi^2}} e^{-\xi\omega_n t}\sin(\omega_n\sqrt{1-\xi^2}) \end{aligned} \tag{10}$$

Thus, the overshoot value is obtained as:

$$V_p = \frac{v_{\text{bus\_max}}}{V_{\text{ref}}} = \frac{P}{C_{\text{bus}} V^2{}_{\text{ref}} \omega_n} e^{\frac{-\xi \cos^{-1}\xi}{\sqrt{1-\xi^2}}} \tag{11}$$

3. DESIGN OF DIGITAL FIR FILTER

As discussed in previous sections, one of the design challenges is the second harmonic on the capacitor voltage. To eliminate this harmonic, a digital FIR filter can be used for the second harmonic. Thus, as shown in Figure 3, using a filter can overcome the second challenge. The filter with identical coefficients 1/N is defined as follows, and its block diagram is presented in Figure 4:

$$H_{\text{FIR}}(z) = \frac{1}{N} + \frac{1}{N} z^{-1} + \ldots + \frac{1}{N} z^{-(N-1)} \tag{12}$$

where N is the filter length, equal to the sampling rate divided by the second harmonic frequency. For instance, for a sampling rate of 480Hz and a second harmonic frequency of 120Hz, N = 4, and for a sampling rate of 360Hz, N = 3. The filter performance is shown in Figure 5, where N \ samples are taken per half-cycle of the grid frequency from the DC link voltage, resulting in a unit gain at low frequency and a notch at the grid's second harmonic frequency.

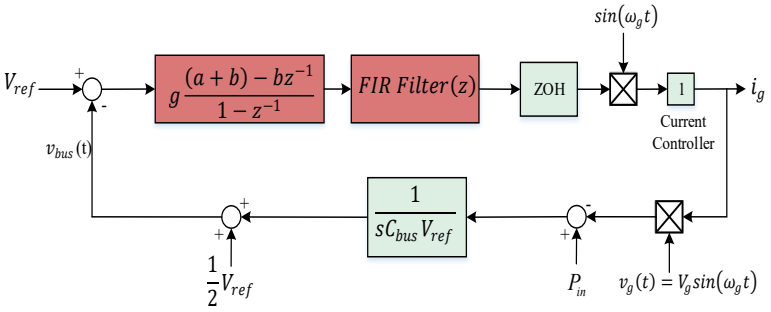

Fig. 3. Control Loop Using Digital FIR Filter

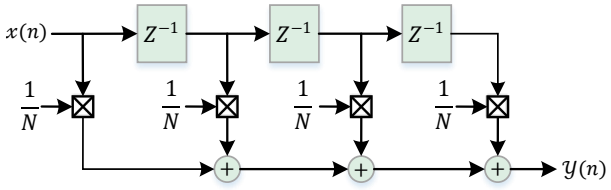

Fig. 4. Block Diagram of Digital FIR Filter

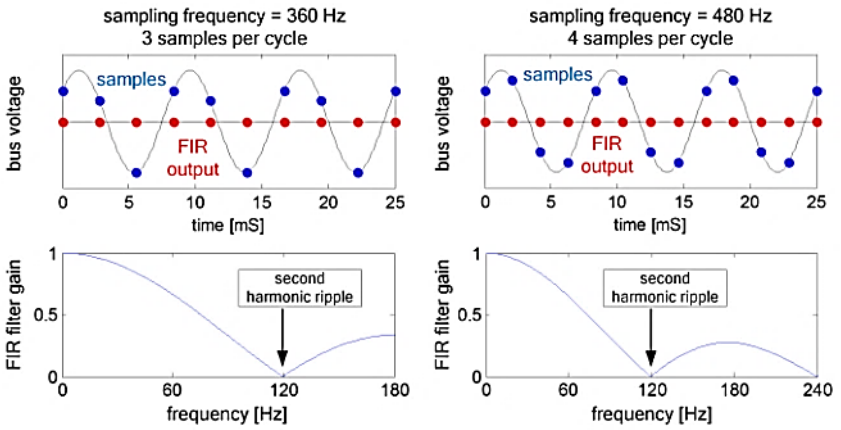

Fig.5. DC Link Capacitor Voltage Filter with Sampling Rates of 480Hz and 360Hz

4. DESIGN AND SIMULATION RESULTS

In the investigated system, a 1Soltech 1STH-250WH solar panel, rated at 250 watts, was used. Table 1 displays the specifications of the simulated system. A proportional-resonant controller with the transfer function $K_p + \frac{2K_r s}{s^2+\omega_1{}^2}$ was used for current control, and an LCL filter with a series resistor with the capacitor was utilized for the output filter, where L_1 is the inverter-side inductor and L_2 is the grid-side inductor.

Table 1. Specifications of the Simulated System

L_1	22mH	**K_p**	5
L_2	13.6mH	**K_r**	40
C	823nF	**f_{sw}**	20KHz
R	33.77Ω	**f_{grid}**	60Hz

The voltage controller was simulated with the specifications shown in Table 2, and the obtained results are presented below.

Table 2. Specifications for the Voltage Controller

V_{ref}=425v	C_{bus}=50μF
$a = 1$	$b = 8$
$N = 1/4$	---

Figure 6 shows the waveform of the DC link capacitor voltage. Figure 7 shows the reference current waveform. Figures 8, 9, and 10 respectively show the waveforms of the inverter output voltage, grid current, and grid voltage. Figure 11 shows the harmonic spectrum, indicating a total harmonic distortion (THD) of 0.47%.

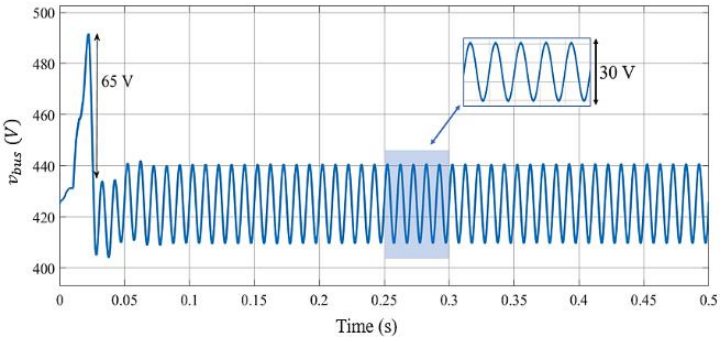

Fig. 6. DC Bus Capacitor Voltage Waveform

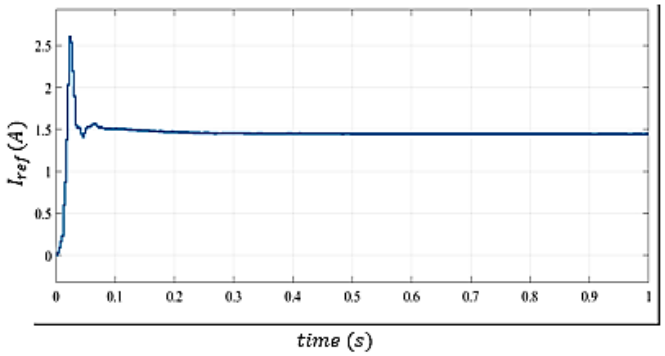

Fig. 7. Reference Current Waveform

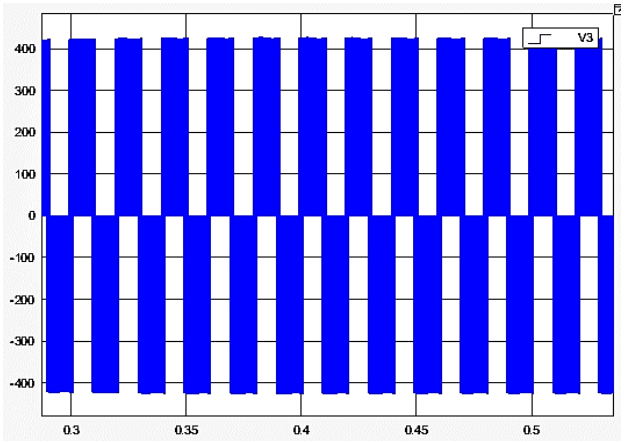

Fig. 8. Inverter Output Voltage Waveform

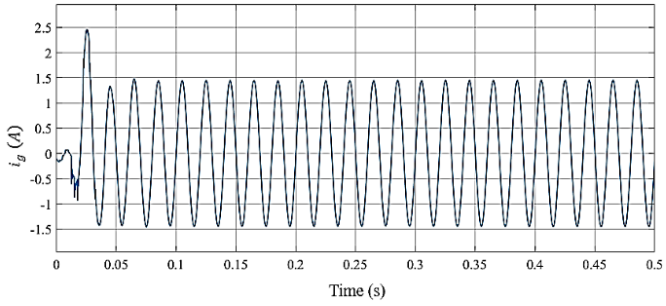

Fig.9. Grid Current Waveform

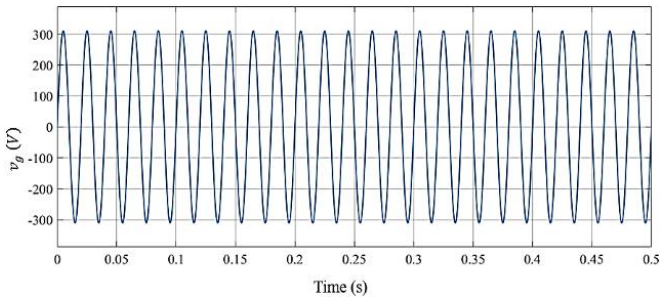

Fig. 10. Grid Voltage Waveform

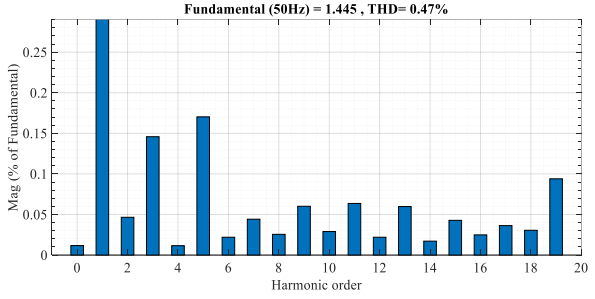

Fig. 11. Harmonic Spectrum of the Grid Current

5. CONCLUSION

This paper examined the challenges in designing a voltage controller for single-phase grid-connected renewable systems. Additionally, a proportional-integral controller was proposed for voltage control, which performed effectively. The entire system was simulated in the MATLAB Simulink environment, using a 50-microfarad isolation capacitor. The overshoot for a 250-watt step was 65 volts, and the THD of the injected current to the grid at 250 watts was approximately 0.47 percent.

Transparency Statement

The data supporting this study are available upon reasonable request to the corresponding author, subject to ethical and confidentiality considerations.

Acknowledgments

We would like to express our gratitude to all individuals who contributed to this project.

Declaration of Interest

The authors declare that they have no competing interests.

Funding

This research received no specific grant from any funding agency, commercial, or not-for-profit sectors.

REFERENCES

[1] Lyeonov, S., Pimonenko, T., Bilan, Y., Štreimikienė, D., & Mentel, G. (2019). Assessment of green investments' impact on sustainable development: Linking gross domestic product per capita, greenhouse gas emissions and renewable energy. Energies, 12(20), 3891. https://doi.org/10.3390/en12203891

[2] Holappa, L. (2020). A general vision for reduction of energy consumption and CO2 emissions from the steel industry. Metals, 10(9), 1117. https://doi.org/10.3390/met10091117

[3] Mikhaylov, A., Moiseev, N., Aleshin, K., & Burkhardt, T. (2020). Global climate change and greenhouse effect. Entrepreneurship and Sustainability Issues, 7(4), 2897-2913. https://doi.org/10.9770/jesi.2020.7.4(21)

[4] Basit, M., Dilshad, S., Badar, R., & Rehman, S. (2020). Limitations, challenges, and solution approaches in grid-connected renewable energy systems. International Journal of Energy Research, 44(6), 4132-4162. https://doi.org/10.1002/er.5033

[5] Vasylieva, T., Lyulyov, O., Bilan, Y., & Štreimikienė, D. (2019). Sustainable economic development and greenhouse gas emissions: The dynamic impact of renewable energy consumption, GDP, and corruption. Energies, 12(17), 3289. https://doi.org/10.3390/en12173289

[6] Kjaer, S. B., Pedersen, J. K., & Blaabjerg, F. (2005). A review of single-phase grid-connected inverters for photovoltaic modules. IEEE Transactions on Industry Applications, 41(5), 1292-1306. https://doi.org/10.1109/TIA.2005.853371

[7] Hu, H., Harb, S., Kutkut, N., Batarseh, I., & Shen, Z. J. (2010). Power decoupling techniques for micro-inverters in PV systems-a review. In 2010 IEEE Energy Conversion Congress and Exposition (pp. 3235-3240). https://doi.org/10.1109/ECCE.2010.5618285

[8] Li, Q., & Wolfs, P. (2008). A review of the single phase photovoltaic module integrated converter topologies with three different DC link configurations. IEEE Transactions on Power Electronics, 23(3), 1320-1333. https://doi.org/10.1109/TPEL.2008.920883

[9] Levron, Y., Canaday, S., & Erickson, R. W. (2016). Bus voltage control with zero distortion and high bandwidth for single-phase solar inverters. IEEE Transactions on Power Electronics, 31(1), 258-269. https://doi.org/10.1109/TPEL.2015.2399431

[10] Karimi-Ghartemani, M., Khajehoddin, S. A., Jain, P., & Bakhshai, A. (2013). A systematic approach to DC-bus control design in single-phase grid-connected renewable converters. IEEE Transactions on Power Electronics, 28(7), 3158-3166. https://doi.org/10.1109/TPEL.2012.2222672